Solid-State Luminescence Hot Paper

International Edition: DOI: 10.1002/anie.201508461
German Edition: DOI: 10.1002/ange.201508461

$B(C_6F_5)_3$: A Lewis Acid that Brings the Light to the Solid State

Max M. Hansmann, Alicia López-Andarias, Eva Rettenmeier, Carolina Egler-Lucas, Frank Rominger, A. Stephen K. Hashmi, and Carlos Romero-Nieto**

Abstract: *The straightforward coordination of the Lewis acid $B(C_6F_5)_3$ to classical, non-emitting aldehydes results in solid-state photoluminescence. Variation of the electronic properties of the carbonyl moieties lead to the modulation of the solid-state emission colors, covering the entire visible spectrum with quantum yields up to 0.64. Steady-state spectroscopy in combination with X-ray diffraction analysis and DFT calculations confirm that intermolecular interactions between the Lewis adducts are responsible for the observed luminescence. Alteration of the latter interactions induces, moreover, remarkable solid-state phenomena such as piezochromism. The versatility and simplicity of our approach facilitate the future development of solid-state emitting materials.*

Solid-state luminescent materials are of utmost importance because of their application in light-emitting diodes (LEDs),[1] lasers,[2] and luminescent sensors.[3] Thus, over the last decades materials research has focused on defining the key factors that lead to the best emission performances. As a result, it is well established that: 1) Ideally in photoluminescent materials, intermolecular interactions must restrict nonradiative relaxation processes, namely, intramolecular rotations.[4] The energy levels can then rearrange, generating extremely efficient photoinduced emission. 2) The presence of halogens, some transition metals, and carbonyl groups must be avoided. Their n–π^* transitions typically promote efficient intersystem crossing and thus deactivate fluorescent decays.[5] These findings have certainly limited the diversity of efficient solid-state emitting materials. Most molecular dyes exhibit reduced or quenched luminescence when the molecular density is increased from diluted solutions to the solid state. This is attributed to intermolecular interactions or intersystem crossings that dissipate the absorbed energy.[6]

Recently, boranes demonstrated to successfully circumvent the aforementioned bottlenecks. Thus, a myriad of chelating four-coordinate organoboron compounds have been reported.[7] Fraser et al. described, for instance, the preparation of organoboranes from 1,3-diketones with extraordinary solid-state photophysical properties[8] (dual room-temperature fluorescence and phosphorescence). In that context, examples of nonchelating boranes are, on the other hand, rather scarce. Bazan et al.[9] reported the possibility to modify the absorption properties of benzothiadiazole-containing architectures by coordination of the $B(C_6F_5)_3$ Lewis acid to the nitrogen atoms of the benzothiadiazole units. The formation of B–N adducts led to a reduction of the optical bandgap and thus to absorption features in the near infrared. Although the coordination properties of $B(C_6F_5)_3$ were reported by Piers et al. years ago,[10] the utilization of this Lewis acid was, until now, restricted to frustrated Lewis pair chemistry[11] and catalysis-related applications.[12] The latter motivated us to investigate the impact of the $B(C_6F_5)_3$ coordination on the photophysical properties of materials capable of strongly interacting with boranes, that is, nonchelating aldehyde-containing architectures.[10]

To conduct a systematic investigation, we designed a series of aldehyde-containing materials meeting the following requirements: a) straightforward preparation, b) gradual variation of the optical bandgap, c) different electronic communication between the π-system and the carbonyl group, and d) the presence of double or triple bonds as unsaturated carbon functional groups. Thus, we designed a series of tolane and stilbene derivatives with electron-donating or -accepting peripheral groups, and a carbonyl moiety in *ortho* or *para* position (compounds **1b–k**; Scheme 1).

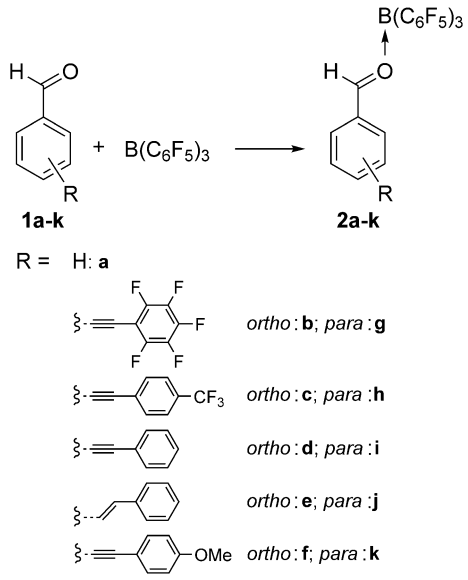

Scheme 1. Preparation of carbonyl–borane adducts **2a–k**.

[*] Dr. M. M. Hansmann, M. Sc. A. López-Andarias, Dr. E. Rettenmeier, Dr. C. Egler-Lucas, Dr. F. Rominger, Prof. Dr. A. S. K. Hashmi, Dr. C. Romero-Nieto
Organisch-Chemisches Institut
Ruprecht-Karls-Universität Heidelberg
Im Neuenheimer Feld 270, 69120 Heidelberg (Germany)
E-mail: hashmi@hashmi.de
carlos.romero.nieto@oci.uni-heidelberg.de
Prof. Dr. A. S. K. Hashmi
Chemistry Department, Faculty of Science, King Abdulaziz University
Jeddah 21589,(Saudi Arabia)

Supporting information for this article is available on the WWW under http://dx.doi.org/10.1002/anie.201508461.

DFT calculations (B3LYP/6-31G + (d) level of theory) show a gradual variation of the HOMO and LUMO frontier orbitals within the *ortho* and *para* series (Figure S1 and Table S1 in the Supporting Information, SI). Moreover, we included the benzaldehyde **1a** as a model compound. The preparation of the tolane and stilbene derivatives was carried out by simple Sonogashira or Suzuki–Miyaura cross-coupling, respectively, from commercially available reactants.

The synthesis of the R-CHO→$B(C_6F_5)_3$ adducts turned out to be highly selective and quantitative; a competing reaction of the borane Lewis acid with the unsaturated double or triple bonds was not observed. Thus, the addition of an equimolar amount of $B(C_6F_5)_3$ to **1a–k** in dichloromethane led instantly to the corresponding borane adducts **2a–k** (see SI). The products were fully characterized by NMR and FTIR spectroscopy, mass spectrometry, elemental analysis, and X-ray diffraction analysis.

First insights into the impact of the $B(C_6F_5)_3$ coordination came from DFT calculations (Figure S1 and Table S1). In all cases, binding of the boron atom leads predominantly to a lower LUMO level and, accordingly, to a reduction of the optical band gap. In turn, the electronic densities rearrange so that the LUMO contains the carbonyl moiety and the HOMO is located on the borane group (Figure 1; and Figures S2–S5).

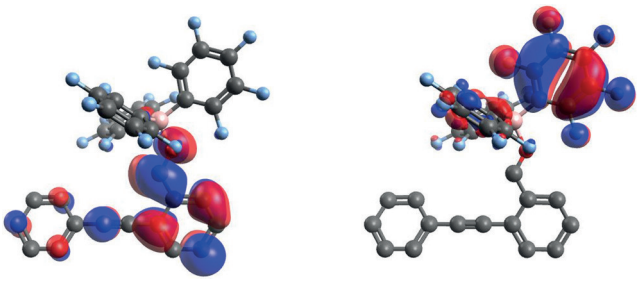

Figure 1. Representative LUMO (left) and HOMO (right) obtained by DFT calculations on the adduct **2d**.

Next, to evaluate the photophysical properties of the borane adducts, we turned our focus to steady-state spectroscopy. In general, carbonyl-containing compounds typically exhibit rather low fluorescence quantum yields (QYs)($\Phi < 0.05$);[13,5] the n-π^* singlet state funnels photoexcited electrons into the π-π^* triplet state, preventing efficient fluorescent decay. Here, we expected the electronic rearrangement caused by the O–B coordination to suppress the aforementioned photoinduced processes, promoting thus improved luminescence. However, dichloromethane solutions of **2a–k** indicated that the O–B coordination has a negligible effect on the spectroscopic features. Namely, the absorption spectra from diluted solutions exhibit identical absorption maxima in the UV range, between 260 and 341 nm (Figures S6 and S7). In turn, emission properties remain unaltered, that is, $\Phi < 0.02$. A different scenario emerged when the concentration was increased above 10^{-5} M.

Model compounds are fundamental to shed light on spectroscopic behaviors. Thus, we first centered our investigations on compound **2a**. Diluted solutions of the latter

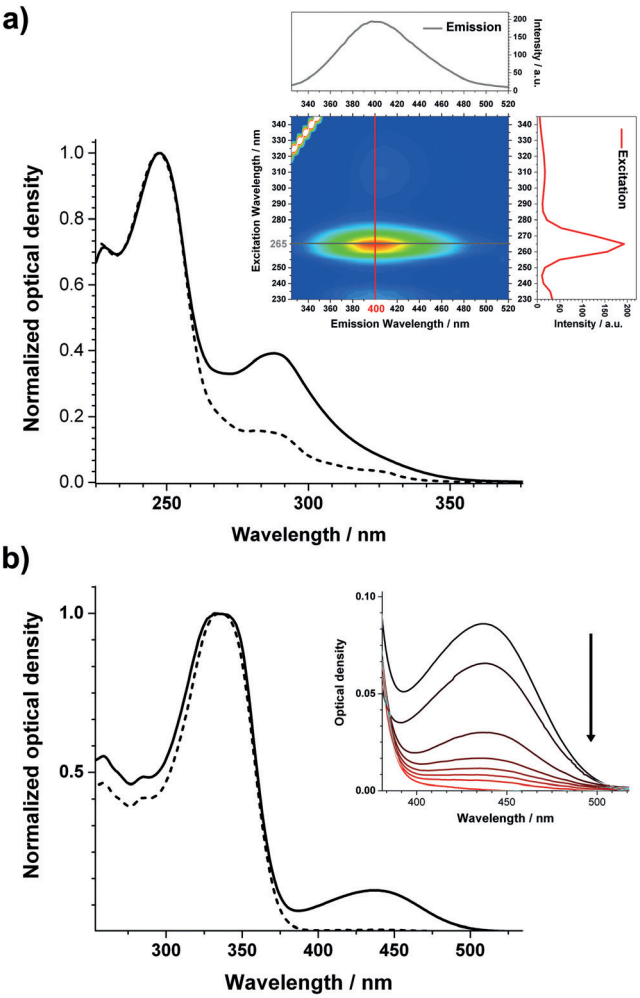

Figure 2. a) Normalized absorption spectra of **2a** from concentrated (solid line) and dilute (dashed line) solutions. Inset: 3D emission spectrum of a concentrated solution of **2a** in dichloromethane; emission (gray) and excitation (red) spectra corresponding to the maxima. b) Representative absorption spectra of **2k** from concentrated (solid line) and dilute (dashed line) solutions. Inset: Gradual fading of the absorption band after the dropwise addition of methanol.

exhibit absorption maxima at 248 and 288 nm (Figure 2a). However, increasing the solution's concentration leads to a new shoulder in the absorption spectrum at 316 nm (Figure 2a). Surprisingly, photoexcitation of the newly formed absorption band gives rise to emissive features that maximize at 400 nm. Three-dimensional steady-state spectroscopy provides better insight into the origin of the new emission band (Figure 2a, inset). Thus, a maximum at 265 nm and a broad band centered at 310 nm appear responsible for the photoluminescence of the benzaldehyde–$B(C_6F_5)_3$ adduct (see Figure 2a, excitation spectrum).

The observation of these new emissive properties from a typically non-emitting carbonyl compound motivated us to continue our studies systematically with substituted benzaldehydes. In all cases, increasing the concentration of **2b–k** induces the formation of a new absorption band of lower energy (Figure 2b and Figures S8–S17). Importantly, this band was found to be stable upon dilution on the exper-

imental time scale (Figure S18). Again, these new emerging absorption bands are responsible for a prominent luminescent process; excitation spectra corroborate the latter (Figures S7–S17). Concentrated solutions exhibit emission maxima that range from 437 to 613 nm, as a function of the different peripheral groups (Figure S19). One rationale infers the formation of aggregates in the ground state, which lead to the newly formed spectroscopic features.

To verify the role of the O–B coordination in the formation of emissive aggregates, we progressively replaced the aldehyde moieties of the adducts **2b–k** with methanol. Thus, when methanol is added dropwise to the concentrated solutions, the new absorption bands gradually disappear (Figure 2b, inset, and Figures S20–S24). The lack of shifts in the absorption maxima is consistent with the formation of discrete aggregates.[14] Massive molecular aggregation would lead to a progressive displacement of the absorption bands as the aldehydes are replaced.

In view of the photoluminescence of the concentrated solutions, we investigated the solid-state spectroscopic properties of **2b–k**. Surprisingly, we found the substituted benzaldehyde–borane adducts to exhibit a strong photoluminescence (Figures S25–S35). It is important to note that neither the free Lewis acid $B(C_6F_5)_3$ nor compounds **1b–k** exhibit any significant emission properties in the solid state. Remarkably, the emission maxima of the borane adducts range through the entire visible spectrum, that is, from 444 nm for **2b** to 625 nm for **2k** (Figure 3a). Thus, the emission maxima are determined by the nature of the peripheral groups. Increasing the electron-donating capacity leads to a red shift of the borane adducts' emission features. The color coordinates (Figure 3b and Table S3) provide additional information on the observed fluorescent colors (Figure 3c). Solid-state fluorescence quantum yields of the borane derivatives differ from 0.64 for **2d** to 0.15 for **2k** (Table S4), presumably due to the stronger donor–acceptor character of the latter adduct.

Overall, emission maxima are bathochromically shifted in the solid state with respect to those of concentrated solutions. The latter indicates the presence of additional intermolecular interactions. Thus, fluorescence decays appear bi-exponential in the solid state (see Table S4).[15]

To investigate the intermolecular interactions in the solid state, we focused on single crystal X-ray analysis (Figure 4a and Figures S36–S40). Analyses of the three-dimensional arrangements reveal a strong preference of the $B(C_6F_5)_3$ moieties to interact with one another. In all cases, the shortest distances are found for F–F interactions between $B(C_6F_5)_3$ and range from 2.83 to 2.94 Å. Thus, the boron center with an increased electronic density, surrounded by highly polarized C_6F_5 groups, drives the intermolecular interactions (Figure 4a and Figures S36–S40). This leads, for example in **2d**,[16] to dimeric structures (Figure 4a). DFT calculations of the latter assembly provide information about the resulting electronic rearrangement (Figure S42). Thus, both the HOMO and LUMO appear to be doubly degenerated; the HOMO is centered on the diborane nucleus, whereas the LUMO is located on both aldehyde moieties.

These observations, together with our spectroscopic investigations, indicate that: 1) The coordination of $B(C_6F_5)_3$

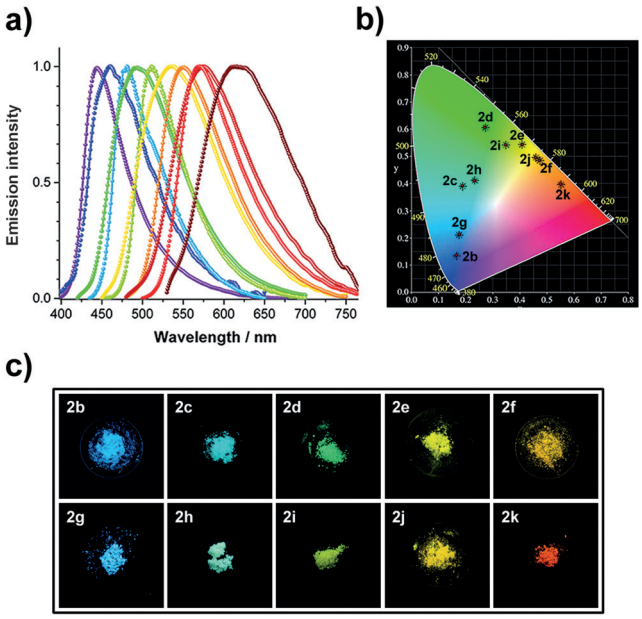

Figure 3. a) Normalized solid-state fluorescence of **2b–k**. b) CIE color coordinates from the solid-state emission of **2b–k**. c) Solid-state photoluminescence of compounds **2b–k**.

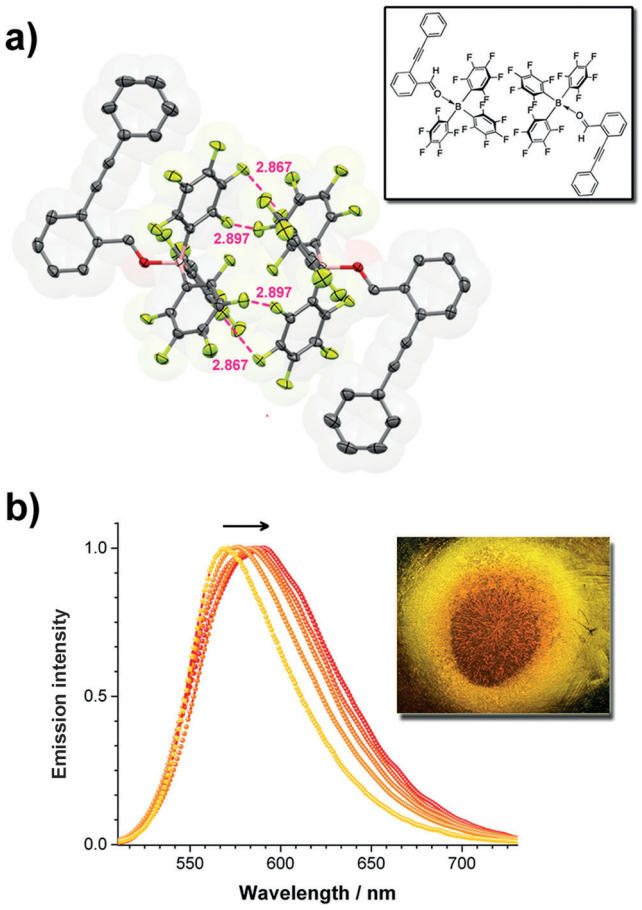

Figure 4. a) Packing of **2d** deduced from X-ray crystallography. Shortest F–F interactions are indicated in pink. b) Changes in the solid-state photoluminescence of **2f** and color change from orange to red (inset) upon increasing pressure.

to carbonyl groups does not prevent radiationless processes in individual aldehyde molecules: diluted solutions do not emit. b) The intermolecular interactions lead to circumvent the nonradiative processes and, ultimately, enable the photoluminescence. It is important to note that after aggregation the energy distribution of the carbonyl–borane adducts is altered (Figure S42) leading to the emissive state. A rationale infers the latter redistribution to be responsible for preventing the radiationless transitions.

Accordingly, altering the intermolecular interactions would modify the photophysical properties of the solid state. To verify our hypothesis, we reproduced our spectroscopic measurements while applying increasing pressure. Compounds with narrower optical band gaps facilitate the identification of batho- or hypsochromic changes. Thus, increasing the pressure on solid **2 f** induced piezochromism, that is, a red shift of the emission maximum from 570 nm to 590 nm (Figure 4 b), which correlates with a color change from orange to red (Figure 4 b, inset). Importantly, when the sample was ground, the original spectroscopic features were regenerated.

In conclusion, we report a straightforward protocol to efficiently turn on the solid-state photoluminescence of typically non-emissive carbonyl materials by simple coordination of the Lewis acid $B(C_6F_5)_3$. Our method appears compatible with materials containing double or triple bonds. Subtle modification of the carbonyl molecules leads to emissive colors that cover the entire visible spectrum with high quantum yields. Intermolecular interactions promoted by $B(C_6F_5)_3$ enable, moreover, intriguing phenomena such as piezochromism. The commercial availability of $B(C_6F_5)_3$ and the simplicity of our method allow the facile preparation of novel materials with enhanced solid-state fluorescence. Investigations on superior carbonyl architectures are currently in progress.

Acknowledgements

C.R.N. and A.L.A. thank the Fonds der chemischen Industrie for a Liebig Grant and a fellowship, respectively. Moreover, C.R.N., A.L.A., and C.E.L. thank Prof. Bunz and the Organisch-Chemisches Institut of the University of Heidelberg for the outstanding support. M.M.H. is grateful to the Fonds der chemischen Industrie for a Chemiefonds scholarship and the Studienstiftung des deutschen Volkes.

Keywords: aldehydes · boranes · fluorescence · piezochromism · solid-state luminescence

How to cite: *Angew. Chem. Int. Ed.* **2016**, *55*, 1196–1199
Angew. Chem. **2016**, *128*, 1212–1216

[1] S. B. Meier, D. Tordera, A. Pertegás, C. Roldán-Carmona, E. Ortí, H. J. Bolink, *Mater. Today* **2014**, *17*, 217.
[2] S. Chénais, S. Forget, *Polym. Int.* **2012**, *61*, 390.
[3] Z. M. Hudson, S. Wang, *Acc. Chem. Res.* **2009**, *42*, 1584.
[4] Y. Hong, J. W. Lam, B. Z. Tang, *Chem. Soc. Rev.* **2011**, *40*, 5361.
[5] J. R. Lakowicz, *Principles of Fluorescence Spectroscopy*, Springer, New York, **2007**.
[6] J. Mei, Y. Hong, J. W. Y. Lam, A. Qin, Y. Tang, B. Z. Tang, *Adv. Mater.* **2014**, *26*, 5429.
[7] a) D. Li, H. Zhang, Y. Wang, *Chem. Soc. Rev.* **2013**, *42*, 8416; b) F. Jäkle, *Chem. Rev.* **2010**, *110*, 3985; c) N. Boens, V. Leena, W. Dehaen, *Chem. Soc. Rev.* **2012**, *41*, 1130; d) S. Yamaguchi, A. Wakamiya, *Pure Appl. Chem.* **2006**, *78*, 1413; e) A. Wakamiya, S. Yamaguchi, *Bull. Chem. Soc. Jpn.* **2015**, *88*, 1357.
[8] G. Zhang, G. M. Palmer, M. W. Dewhirst, C. L. Fraser, *Nat. Mater.* **2009**, *8*, 747.
[9] a) G. C. Welch, R. Coffin, J. Peet, G. C. Bazan, *J. Am. Chem. Soc.* **2009**, *131*, 10802; see also: b) G. C. Welch, G. C. Bazan, *J. Am. Chem. Soc.* **2011**, *133*, 4632; c) P. Zalar, Z. H. Henson, G. C. Welch, G. C. Bazan, T. Q. Nguyen, *Angew. Chem. Int. Ed.* **2012**, *51*, 7495; *Angew. Chem.* **2012**, *124*, 7613.
[10] D. J. Parks, W. E. Piers, M. Parvez, R. Atencio, M. J. Zaworotko, *Organometallics* **1998**, *17*, 1369.
[11] D. W. Stephan, G. Erker, *Angew. Chem. Int. Ed.* **2010**, *49*, 46; *Angew. Chem.* **2010**, *122*, 50.
[12] a) X. Yang, C. L. Stern, T. J. Marks, *J. Am. Chem. Soc.* **1994**, *116*, 10015; b) D. J. Parks, W. E. Piers, *J. Am. Chem. Soc.* **1996**, *118*, 9440; For the unique properties of $B(C_6F_5)_3$, see the following reviews: c) W. E. Piers, T. Chivers, *Chem. Soc. Rev.* **1997**, *26*, 345; d) W. E. Piers, *Adv. Organomet. Chem.* **2004**, *52*, 1; e) G. Erker, *Dalton Trans.* **2005**, 1883; f) W. E. Piers, A. J. V. Marwitz, L. G. Mercier, *Inorg. Chem.* **2011**, *50*, 12252.
[13] a) G. G. Guilbault, *Practical Fluorescence*, *2nd ed.*, M. Dekker, New York, **1990**; b) R. P. Haugland, *Handbook of Fluorescent Probes and Research Products*, Molecular Probes, Eugene, **2002**; c) B. Valeur, *Molecular Fluorescence*: *Principle and Applications*, Wiley-VCH, Weinheim, **2002**; d) J. Malkin, *Photophysical and Photochemical Properties of Aromatic Compounds*, CRC, Boca Raton, **1992**; e) *Handbook of Organic Photochemistry and Photobiology* (Eds.: W. M. Horspool, P.-S. Song), CRC, Boca Raton, **1995**.
[14] B. Z. Tang, A. Qin, *Aggregation-Induced Emission: Fundamentals*, Wiley-VCH, Weinheim, **2013**.
[15] Fluorescence decays in the solid state are generally multi-exponential due to the presence of multiple deactivation pathways.
[16] CCDC 1419191, 1419192, 1419193, 1419194, 1419195 and 1419196 contain the supplementary crystallographic data for this paper. These data can be obtained free of charge from The Cambridge Crystallographic Data Centre via www.ccdc.cam.ac.uk/data_request/cif.

Received: September 9, 2015
Published online: December 10, 2015

